# Indentation Size Effect in Bulk Metallic Glass

Jae-il Jang,[1,*] Byung-Gil Yoo,[1] Yong-Jae Kim,[1] Jun-Hak Oh,[1] In-Chul Choi,[1] Hongbin Bei[2,*]

[1] Division of Materials Science and Engineering, Hanyang University, Seoul 133-791, Korea

[2] Materials Science and Technology Division, Oak Ridge National Laboratory, Oak Ridge, TN 37831-6115, USA

* Corresponding authors.

Electronic address: jijang@hanyang.ac.kr (J.-i. Jang), beih@ornl.gov (H. Bei)

## Abstract

We systematically explored indentation size effect (ISE, that is not expected to occur in non-crystalline materials due to the absence of dislocations and strain hardening) in bulk metallic glass (BMG). A series of nanoindentation experiments with different indenters result in somewhat surprising observations that clear ISE does indeed exist in the BMG and even it can be described by the ISE model for crystalline materials. The results are discussed in terms of possible mechanisms responsible for the ISE in BMG.

Key words: Nanoindentation; bulk amorphous materials; hardness; size effect.

With accelerated advance in small-scale mechanical testing techniques over the past two decades, fundamental knowledge about the size effects on strength and plasticity of crystalline materials has become remarkably widened. A representative example of such size effects is the so-called indentation size effect (ISE), which is manifested as an increase in hardness $H$ with decreasing impression size $A$ or indentation depth $h$ or peak load $P_{max}$ (see recent review by Pharr et al. [1]). While the ISE was often observed during nanoindentation experiments made with a geometrically self-similar pyramidal indenter (such as commonly-used Berkovich and Vickers indenter), the size-dependency of the hardness $H$ (defined as $P_{max}/A$) could not be explained by continuum plasticity concepts for which there is no inherent material length scale and thus the $H$ should be independent of the impression size $A$. To analyze this intriguing phenomenon, early works on the ISE mostly adopted strain gradient plasticity theory (that is, geometrically necessary dislocations (GNDs) would nucleate for accommodating plastic strain gradients in bending or indentation and thus would increase the strength) and proposed possible relationship between the GNDs and the ISE [1]. The most popular mechanism-based ISE model was established by Nix and Gao [2], who considered the density of GNDs (generated by a sharp indenter) together with a Taylor's dislocation strengthening model. In the Nix-Gao model [2], the relation between the indentation hardness ($H$) and the indentation depth ($h$) can be simply described as

$$\frac{H}{H_0} = \sqrt{1 + \frac{h^*}{h}} \tag{1}$$

where $h^*$ is a characteristic length and $H_0$ is the macroscopic indentation hardness (when $h$ is much greater than $h^*$). The $h^*$ is given as

$$h^* = \frac{81}{2} b\alpha^2 \cot^2\theta \cdot \left(\frac{G}{H_0}\right)^2, \tag{2}$$

where $b$ is the Burgers vector, $\alpha$ is a geometric constant, $\theta$ is the half-cone angle, and $G$ is the shear modulus. Since the linear relation between $(H)^2$ and $(1/h)$ in Eq. (1) successfully predicted the experimental indentation hardness data for many crystalline materials, the Nix-Gao model has been applied extensively [1].

Since the Nix-Gao model is based on dislocation strengthening, one may imagine that the ISE does not occur in the materials which have non-crystalline (amorphous) structure or show no strain hardening. An interesting example of such materials is bulk metallic glasses (BMGs), which has recently attracted many interests from both scientific and technological viewpoints. The BMGs do not contain crystalline defects such as dislocations so that dislocation-mediated plasticity does not occur in those materials. Instead, the BMGs exhibit the unique nature of plastic deformation; at ambient temperature, plastic strain is highly localized into very narrow 'shear bands' within which collective atomic rearrangements called shear transformation zones (STZs, that are the fundamental carriers of plasticity in metallic glasses) are densely populated [3]. This shear-band-mediated plasticity can hardly lead to expectation of the size-dependent hardness in BMGs, however some researchers have reported the ISE-like behavior in Zr-, Pd-, and Fe-based BMGs [4-11].

While limited literatures are available to report the possibility of ISE phenomenon in BMGs, much more efforts have been devoted into different type of the size effect on strength of BMGs, i.e., the sample size effect (SSE) on strength from uniaxial compression/tension tests of nano-/micro-pillar samples [12-25]. However, there is no consensus on the SSE of BMGs; some researchers showed 'smaller is stronger [12,13,23-25],' whereas others reported the opposite softening trend [14,19].' It has been also proposed that the strength of BMG is actually size-independent [15-18,20-22]. It is noteworthy that there are clear differences in the mechanical

environment between nanoindentation and uniaxial nano-/micro-pillar tests, which may lead to the different mechanisms for the ISE and SSE. First, unlike pillar tests, the plasticity (and fracture) in highly-stressed volume underneath the indenter is constrained by surrounding materials, and thus catastrophic failure does not occur during indentation. Second and more importantly, complex 3-dimensional stress/strains and strain gradients are developed in the sample during indentation whereas the uniaxial pillar sample experiences almost no strain gradient. Therefore, unlike the ISE, the SSE cannot be explained by the strain-gradients. Even for crystalline materials in which the ISE and SSE usually follow the same trend of 'the smaller, the stronger,' different mechanisms have been developed; i.e. strain-gradients model for the ISE and dislocation starvation model for the SSE, as reviewed in [26].

In this work, we systematically analyzed the possibility of ISE in a Zr-based BMG through nanoindentations with a series of three-sided pyramidal indenters having different indenter angles from 35.3° to 70°. The purpose of this letter is to report our somewhat surprising observations that clear ISE does indeed exist in the BMG and can be described by the Nix-Gao rule originally suggested for crystalline materials [2].

The bulk metallic glass examined in this work is a Zr-based BMG, $Zr_{52.5}Cu_{17.9}Ni_{14.6}Al_{10}Ti_5$ (referred to as Vit 105), which was produced in the form of a rod having diameter and length of about 7 and 70 mm respectively. Non-crystalline structure of the sample was confirmed by the absence of crystalline peak in X-ray diffraction pattern (shown elsewhere [27]) analyzed using D/MAX-2500 (Rigaku-Denki, Japan). Nanoindentation experiments were performed using a Nanoindenter-XP (MTS Corp., Oak Ridge, TN) at various loads in the range from 5 to 500 mN. Four different triangular pyramidal indenters having centerline-to-face angles, $\psi$, of 35.3° (cube-corner), 50°, 65.3° (Berkovich), and 70° were employed. The accuracy of the angle was reported

by the manufacturer to be within ± 0.15°. In all nanoindentation experiments, the tests were performed at a constant indentation strain rate of 0.05 /s, and thermal drift was maintained below 0.05 nm/s. All the hardness impressions were imaged using a field-emission scanning electron microscopy (SEM), JSM-6330F (JEOL Ltd., Tokyo, Japan) to measure the actual area of the contact. The topological feature of the indented surface was also identified by an atomic force microscopy (AFM), XE-100 (Park Systems, Suwon, Korea).

**Figure 1** shows representative examples of load–displacement (*P*-*h*) curves recorded during nanoindentation experiments performed at various peak loads ($P_{max}$) up to 500 mN (except for the sharpest case of 35.3° in which the highest peak load was set to be 200 mN to avoid a tip breaking at high loads). As seen in the figure, the loading portion of the *P*-*h* curves obtained at different $P_{max}$ overlapped one another perfectly, proving that the tests were remarkably reproducible. In addition, it is evident that, for a given $P_{max}$, a sharper indenter (i.e., an indenter having a smaller angle) produced a larger peak-load displacement ($h_{max}$), implying that a sharper indenter induces greater stresses and strains in the material due to the larger volume of displaced material [28-32].

A beauty of nanoindentation technique is that one can estimate the hardness and effective modulus only by *P*-*h* curve analysis without observation of indentation impression. The most popular way for this analysis is Oliver-Pharr method [33] that has been also used for calculating BMG hardness in most of the previous works reporting the ISE-like behavior of BMGs [4-11].

In the present work, however, we have not adopted the Oliver-Pharr method for two reasons. First, in BMG samples, severe material pile-up is usually observed around indentation impression. Such pile-up is not taken into consideration in the Oliver-Pharr method, and thus can induce an overestimation of the calculated hardness. In this regard, it is interesting to note that

recently Charleux et al. [34] reported more pronounced pile-up at smaller displacement in nanoindentations of Virtoly-1 BMG. If this works, the amount of pile-up-induced overestimation may be greater at smaller depth, which can result in the ISE-like trend and even can bring a question; is the reported ISE-like behavior an artifact related to miscalculations of the hardness? To clarify this issue, here the pile-up amount was evaluated through AFM analysis (see **Figure 2**). It was revealed that, while the ratio of the pile-up height ($h_{\text{pile-up}}$) to the maximum displacement ($h_{\text{max}}$), $h_{\text{pile-up}}/h_{\text{max}}$, for the Berkovich indenter (centerline-to-face angle $\psi$ = 65.3°) increased with reducing the peak load (which is in good agreement with Charleux et al.'s results [34]), the opposite trend was observed for the cube-corner indenter ($\psi$ = 35.3°). This inconsistent trends (possibly due to the increased influence of friction for a sharper indenter) may make the analysis of hardness variation more complex.

Second, in the Oliver-Pharr method [33], the correlation constant $\beta$ (that relates stiffness $S$ to area $A$ in the Oliver-Pharr method) is important for determining the area function and thus the hardness. However, the proper $\beta$ is known only for the commonly-used Berkovich indenter (as a constant of 1.034 [33]), and the dependency of the $\beta$ value on the indenter angle is still unclear [30], which may lead miscalculations of the hardness data for other indenters used in this study and thus make it difficult to directly compare the hardness data from different indenters.

To overcome these difficulties and obtain accurate hardness values, we have directly measured the impression size $A$ from a large number of SEM images (see Supplementary Material), and then obtained the hardness according to the relation $H = 4P/(3\sqrt{3}a^2)$ where $a$ is the averaged length measured from the center of triangular impression to the corner. The variation in hardness is summarized as a function of displacement in **Figure 3a** where, very interestingly, ISE is clearly observed for all used indenters. It should be noted that, although the hardness for a

sharper indenter appears greater at a given displacement $h$, the hardness measured with different indenters cannot be directly compared for a fixed $h$. This is simply because, at a given $P_{max}$, the $h$ becomes deeper for a sharper indenter.

Because all used indenters yielded the ISE, we have attempted to examine whether the ISE can be described according to Eq. (1), i.e., the Nix-Gao model. **Figure 3b** shows the plots of the square of hardness ($H^2$) obtained from SEM images against the reciprocal of the indentation depth ($1/h$). High linearity between $H^2$ and $1/h$ is seen for all used indenters. One of the interesting predictions of the Nix-Gao model is that there is a strong dependence of the hardness behavior on the indenter angle. According to Eqs. (1) and (2), it is apparent that the slope of the linear relation between $H^2$ and $1/h$ should rely on $\cot^2\theta$, which varies by an order of magnitude depending on one's choice of tip. To relate the conical indentation used for Eqs. (1) and (2) to triangular pyramidal indentation in this work, it is useful to make the normal assumption that similar behavior is obtained when the angle of the cone gives the same area-to-depth ratio as the pyramid, which gives the half-cone angle $\theta$ as $\theta = \tan^{-1}(\sqrt{\frac{3\sqrt{3}}{\pi}}\tan\psi)$ where $\psi$ is the centerline-to-face angle. Thus, $\psi$ of 35.3°, 50°, 65.3°, 70° is corresponding to $\theta$ of 42.3°, 56.9°, 70.3° and 74.2° respectively. In **Figure 3c**, the slopes of the straight lines in Figure 3b are plotted against $\cot^2\theta$. Somewhat surprisingly, the plot has very high linearity, implying that the Nix-Gao model indeed agrees very well with the indentation data for a wide range of indenter angles.

Now, important questions one may raise are 'why does the ISE exist for non-crystalline materials?' and 'how can the ISE be fitted by the Nix-Gao model?' While the detailed mechanisms are still far from complete understanding, the previous suggestions in the limited works reporting the ISE-like behavior [4-11] can be roughly categorized into three groups (to our best knowledge). First group [4,7] is the models constructed in a way very analogous to that used

in the Nix-Gao model; the mechanisms proposed by Lam and Chong [4] and recently Yang *et al*. [7] have also adopted the perspective of strain gradient plasticity, and only difference between their models and the Nix-Gao model is that they used the concept of the non-crystalline flow defects instead of the dislocations. Basic assumption in their theories is that the plasticity induced by strain gradient should be accommodated by 'geometrically necessary' flow defects (either shear clusters [4] or excess free volumes [7]), which can be given as

$$H \propto \sqrt{V_S + V_G} \tag{3}$$

where $V_S$ and $V_G$ are density of the statistically-stored defects and geometrically-necessary defects. Therefore, the increased density of the defects at shallow indentation depth is mainly responsible for the ISE in a BMG, as the increase in the geometrically necessary dislocations is in the Nix-Gao model. However, this scenario may not be reasonable, simply because the increase in the glass defects (e.g., excess free volume [3]) would not induce the hardening but the softening in metallic glass [27,35,36].

Second group of the previous suggestions [5,8] is focused on the strain softening [27,35,36] and the hardness dependence on the strain rate imposed during the indentation. Van Steenberge et al. [8] argued that, for a given strain rate, the continuous accumulation of excess free volume during deformation can cause strain softening at large penetration depth and this softening is the source of the ISE. Then, they established a relationship between the hardness and the strain rate based on the classical metallic glass flow equations developed by Spaepen [37] and then Argon [38]:

$$H(\approx 3\sqrt{3}\tau) \propto \sinh^{-1}(\alpha\dot{\gamma}/c_f) \tag{4}$$

where $\tau$ is the shear stress, $\alpha$ is constant, $\dot{\gamma}$ is the shear strain rate, and $c_f$ is the concentration of flow defects. Based on this relation, they argued that, as the indentation strain rate, $d\varepsilon_i/dt = h^{-}$

[1](d$h$/d$t$) [8,31], is diminishing during indentation testing under constant loading rate (d$P$/d$t$), the high indentation stain rate at shallow depth can induce an increase in hardness [8]. However, this possibility could be excluded in the present study because all indentation experiments were performed under constant strain rate instead of constant loading rate. It is seen in **Figure 4** that the strain rate was maintained as constant of 0.05 /s. Another shortcoming in this argument is that the strain softening equation did not take into consideration the geometrical self-similarity of a sharp indenter. From a classical contact mechanics perspective, the stress (or hardness) and the strain underneath a sharp indenter should not vary during indenter penetration. Therefore, in their result, the hardness change is the experimentally-obtained result (or output) rather than controllable input parameter. Thus, this hypothesis can be largely viewed as empirical rather than analytical.

Third group is considering the influences of the surface effect (including residual stress and friction) [6,9-11] as the main cause of the possible ISE in BMG. However, since they did not account for the strain gradient induced by a self-similar indenter, there is no way to explain the angle effect which is very clear in this study.

Collectively, we reach the conclusion that the ISE phenomenon observed in the present work cannot be explained by any group of existing models and should be interpreted in different ways. A new possibility we suggest here is that the occurrence of the shear transformation zones (STZs) [3] might be controlled by the indentation size or the volume of indentation-induced elastic/plastic deformation. For shallow indentations, the highly-stressed volume underneath the indenter is probably too small to have sufficient population of the STZs (that can evolve into the highly active shear bands which being able to accommodate the plastic deformation) and thus the shear bands are forced to operate at a particular location, whereas deep indentations produce

large volume of deformation and thus higher activities of STZs and the shear bands. In this regard, higher hardness might be observed for low-load indentations, because the glass is demanded to shear in particular locations. Additionally, this hypothesis can conceivably explain the angle effect on hardness (i.e., seemingly higher hardness for a sharper indenter as shown in Figure 3a and 3b) in a qualitative manner. For a given $h$ (not for a given $P_{max}$), a sharper indenter having smaller $\theta$ (or $\psi$) produces a smaller contact radius $a$ and thus a smaller volume of highly-stressed or plastic zone (that is often considered to be proportional to $a^3$; for example, $2\pi a^3/3$ in the Nix-Gao model). Therefore, at a given $h$, the lower activities of STZs and the higher hardness may be expected for a sharper indenter, which is in agreement with the trend in the present work.

Before closing, it is constructive to consider the effect of 'volume' size from a perspective of the potential energy landscape (PEL). Harmon *et al*. [39] revealed that the kinetics for anelastic-to-plastic transition in metallic glasses can be separated into slow α and fast β relaxation process that are related to irreversible and reversible hopping respectively. From this perspective, with decreasing 'volume,' the number of α events increases but their amplitude decreases, both of which are strongly dependent on the size and density of isolated STZs since the events may be directly linked to the collapse of the STZ-matrix coherency condition. In contrast, the amplitude of reversible β events is more or less independent of the volume size.

This research was supported by Basic Science Research Program through the National Research Foundation of Korea (NRF) funded by the Ministry of Education, Science and Technology (No. 2010-0025526). The research at ORNL (H.B.) was sponsored by the U.S. Department of Energy, Office of Basic Energy Sciences, Materials Sciences and Engineering Division. We thank Prof. W.D. Nix and anonymous reviewer for the valuable comments.

## References


1. Pharr GM, Herbert EG, Gao Y. Annu. Rev. Mater. Res. 2010;40:271.
2. Nix WD, Gao H. J. Mech. Phys. Solids 1998;46:411.
3. Schuh CA, Hufnagel TC, Ramamurty U. Acta Mater. 2007;55:4067.
4. Lam DCC, Chong ACM. Mater. Sci. Eng. A 2001;318:313.
5. Concustell A, Sort J, Alcalá G, Mato S, Gebert A, Eckert J, Baró MD. J. Mater. Res. 2005;20:2719.
6. Manika I, Maniks J. Acta Mater. 2006;54:2049.
7. Yang F, Geng K, Liaw PK, Fan G, Choo H. Acta Mater. 2007;55:321.
8. Van Steenberge N, Sort J, Concustell A, Das J, Scudino S, Surinach S, Eckert J., Baró MD. Scripta Mater. 2007;56:605.
9. Li N, Chan KC, Liu L. J. Phys. D: Appl. Phys. 2008;41:155415.
10. Li N, Liu L, Chan KC. J. Mater. Res. 2009;24:1693.
11. Li N, Liu L, Chan KC, Chen Q, Pan J. Intermetallics 2009;17:227.
12. Lee CJ, Huang JC, Nieh TG. Appl. Phys. Lett. 2007;91:161913.
13. Zheng Q, Cheng S, Strader JH, Ma E, Xu J. Scripta Mater. 2007;56:161.
14. Huang YJ, Shen J, Sun JF. Appl. Phys. Lett. 2007;90:081919.
15. Volkert CA, Donahue A, Spaepen F. J. Appl. Phys. 2008;103:083539.
16. Schuster BE, Wei Q, Hufnagel TC, Ramesh KT. Acta Mater. 2008;56:5091.
17. Dubach A, Raghavan R, Löffler JF, Michler J, Ramamurty U. Scripta Mater. 2009;60:567.
18. Wu XL, Guo YZ, Wei Q, Wang WH. Acta Mater. 2009;57:3562.
19. Wu Y, Li HX, Chen GL, Hui XD, Wang BY, Lu ZP. Scripta Mater. 2009;61:564.

20. Chen CQ, Pei YT, De Hosson JThM. Phil. Mag. Lett. 2009;89:633.
21. Bei H, Lu ZP, Shim S, Chen G, George EP. Metall. Mater. Trans. A 2010;41:1735.
22. Chen CQ, Pei YT, De Hosson JThM. Acta Mater. 2010;58:189.
23. Lee CJ, Lai YH, Huang JC, Du XH, Wang L, Nieh TG. Scripta Mater. 2010;63:105.
24. Jang D, Greer JR. Nature Mater. 2010;9:215.
25. Bharathula A, Lee SW, Wright WJ, Flores KM. Acta Mater. 2010;58:5789.
26. Nix WD, Greer JR, Feng G, Lilleodden ET. Thin Solid Films 2007;515:3152.
27. Yoo BG, Park KW, Lee JC, Ramamurty U, Jang JI. J. Mater. Res. 2009;24:1405.
28. Jang JI, Lance MJ, Wen S, Pharr GM. Appl. Phys. Lett. 2005;86:131907.
29. Jang JI, Lance MJ, Wen S, Tsui TY, Pharr GM. Acta Mater. 2005;53:1759.
30. Strader JH, Shim S, Bei H, Oliver WC, Pharr GM. Philos. Mag. 2006;86:5285.
31. Jang JI, Yoo BG, Kim JY. Appl. Phys. Lett. 2007;90:211906.
32. Jang JI, Pharr GM. Acta Mater. 2008;56:4458.
33. Oliver WC, Pharr GM. J. Mater. Res. 1992;7:1564.
34. Charleux L, Gravier S, Verdier M, Fivel M, Blandin JJ. Mater. Sci. Eng. A 2008;483-484:652.
35. Bei H, Xie S, George EP. Phys. Rev. Lett. 2006;96:105503.
36. Yoo BG, Kim YJ, Oh JH, Ramamurty U, Jang JI. Scripta Mater. 2009;61:951.
37. Spaepen F. Acta Metall. 1977;25:407.
38. Argon AS. Acta Metall. 1979;27:47.
39. Harmon JS, Demetrious MD, Johnson WD, Samwer K. Phys. Rev. Lett. 2007;99:135502.

## List of Figures

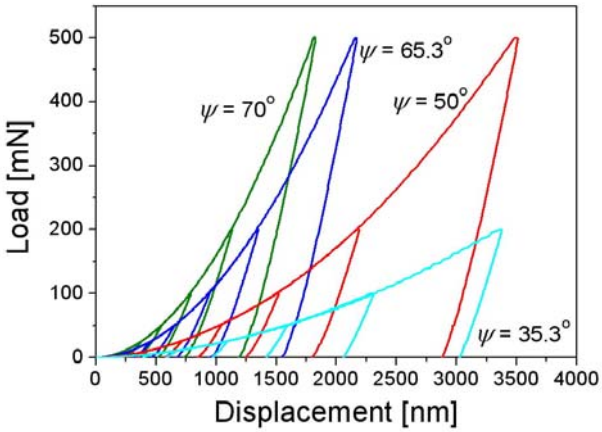


FIG. 1. Jae-il Jang et al.

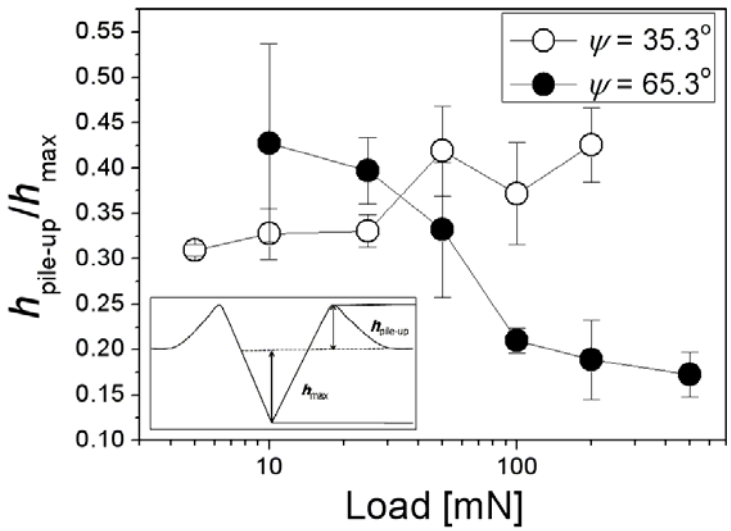


FIG. 2 Jae-il Jang et al.

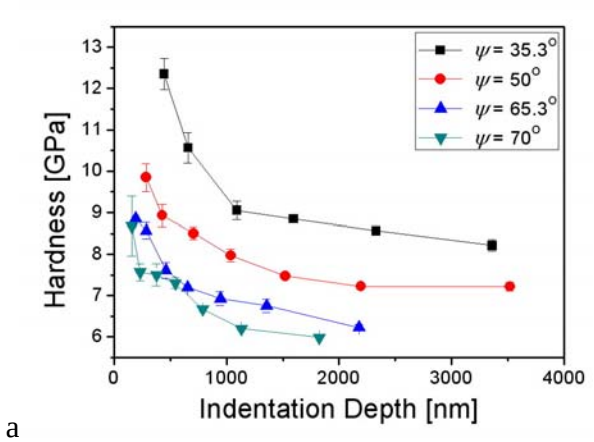


a

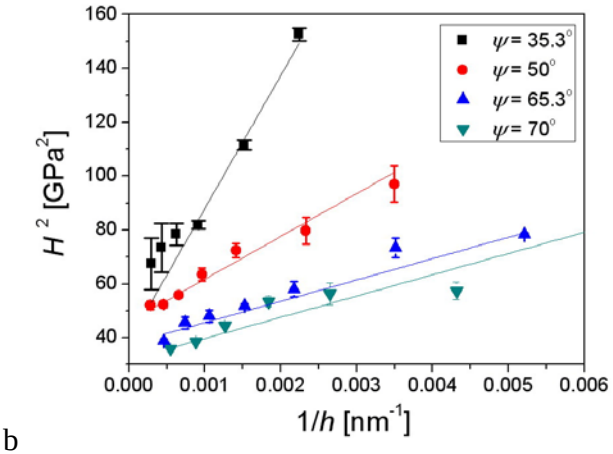


b

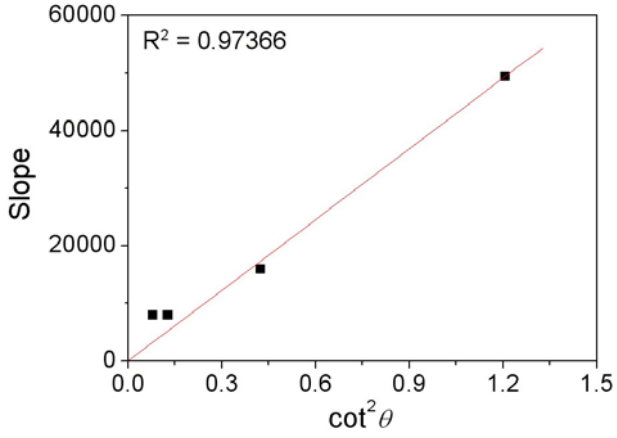


c

FIG. 3. Jae-il Jang et al.

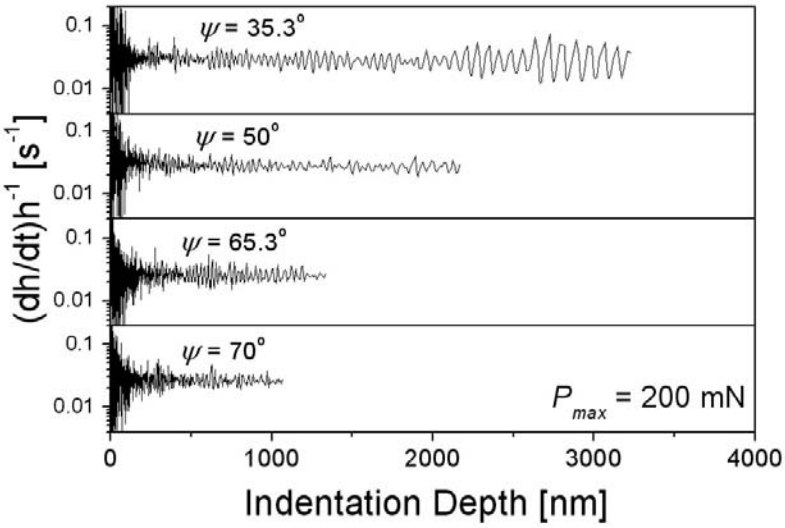


FIG. 4. Jae-il Jang et al.